Molecular Cell, Volume *81*

Supplemental Information

Structural analysis of RIG-I-like receptors reveals ancient rules of engagement between diverse RNA helicases and TRIM ubiquitin ligases

Kazuki Kato, Sadeem Ahmad, Zixiang Zhu, Janet M. Young, Xin Mu, Sehoon Park, Harmit S. Malik, and Sun Hur

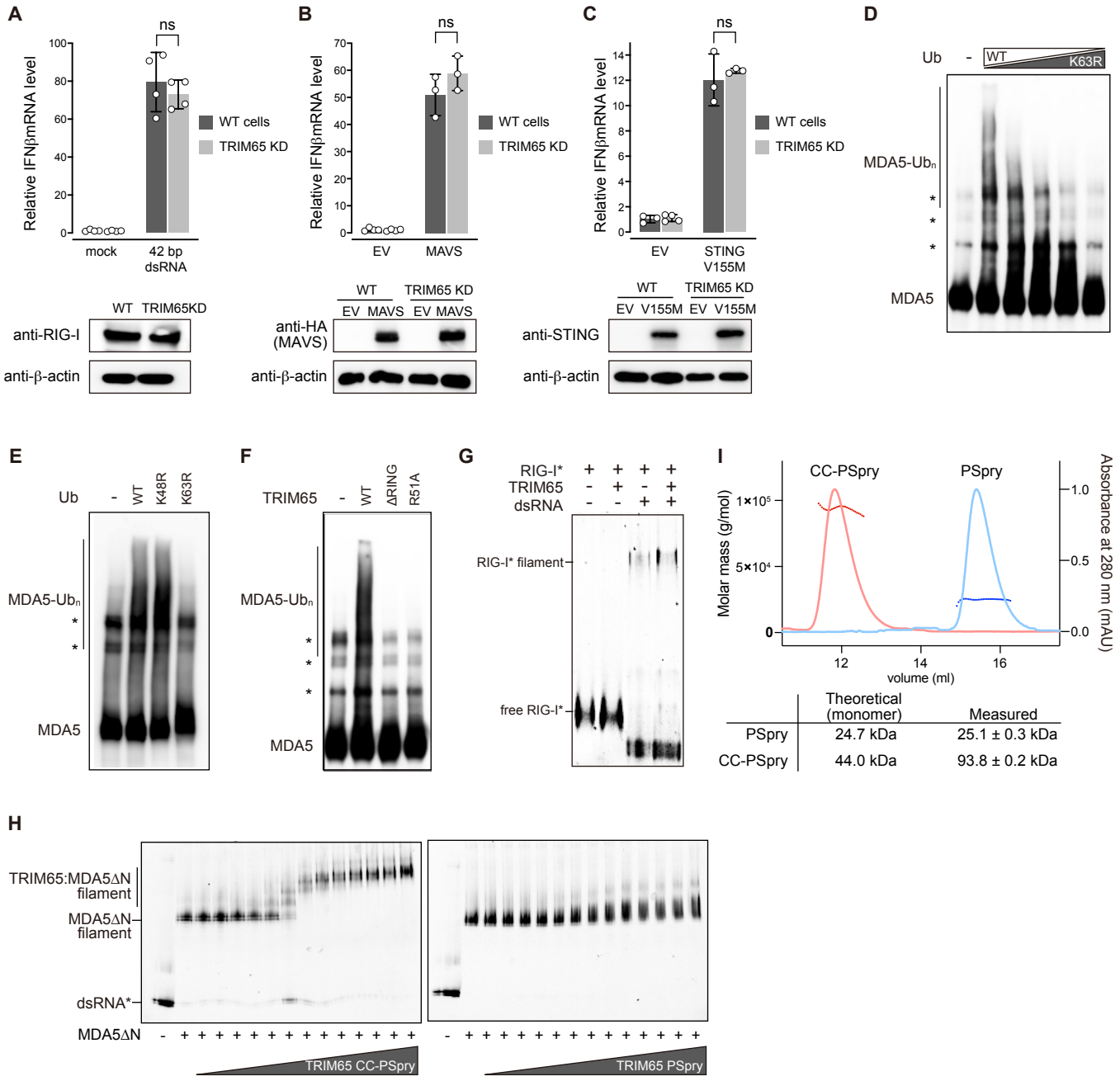

Figure S1. TRIM65 recognizes filamentous MDA5 and conjugates K63-Ubn, Related to Figure 1

(A-C) Relative signaling activity of RIG-I (A), MAVS (B) and STING (B) in WT and TRIM65 KD 293T cells. Endogenous RIG-I was stimulated with 42 bp dsRNA with a 5′-triphosphate group (5′-ppp, 50 ng), which is known to specifically activate RIG-I (Cadena et al., 2019). MAVS and STING pathways were activated by ectopic expression of wild-type MAVS (25 ng) and a constitutively active variant (V155M) of STING (0.75 μg) (Jeremiah et al., 2014). Data are mean ± SD (n=3-4), and *P* values were calculated by two-tailed t-test (ns, not significant; *P*>0.1).

(D) In vitro ubiquitination assay of MDA5 with an increasing ratio of K63R to wild-type Ub. Total concentration of Ub was kept constant at 20 μM. All reactions contained 1012 bp dsRNA (2 ng/μl). Reactions were performed as in Figure 1C and were analyzed by anti-MDA5 western blot.

(E) In vitro ubiquitination assay of MDA5 with WT, K48R or K63R Ub (20 μM).

(F) In vitro ubiquitination assay of MDA5 using wild-type TRIM65, ΔRING or R51A. R51 in TRIM65 corresponds to a conserved E2 binding residue in RING domains (Metzger et al., 2014).

(G) Native gel mobility shift assays to test RIG-I:TRIM65 interaction. Fluorescein-labeled (*) full-length RIG-I (600 nM) was incubated with TRIM65 (300 nM) in the presence and absence of 112 bp dsRNA (4 ng/μl). Fluorescein fluorescence was used for gel imaging. The result shows no binding between RIG-I and TRIM65, with or without dsRNA.

(H) Comparison between TRIM65 CC-PSpry and PSpry for MDA5 filament binding. MDA5ΔN filament was formed by mixing Cy5-labeled (*) 112 bp dsRNA (1 ng/μl) and MDA5ΔN (250 nM). The filament was then incubated with an increasing concentration of CC-PSpry or PSpry (1.57-6400 nM), and the complex formation was analyzed by native PAGE. See Figure 1F for quantitation of binding.

(I) Size-exclusion chromatography (SEC) coupled multi-angle light scattering (MALS) analysis of TRIM65 CC-PSpry and PSpry. Measured and theoretical molecular weights of the proteins are indicated below.

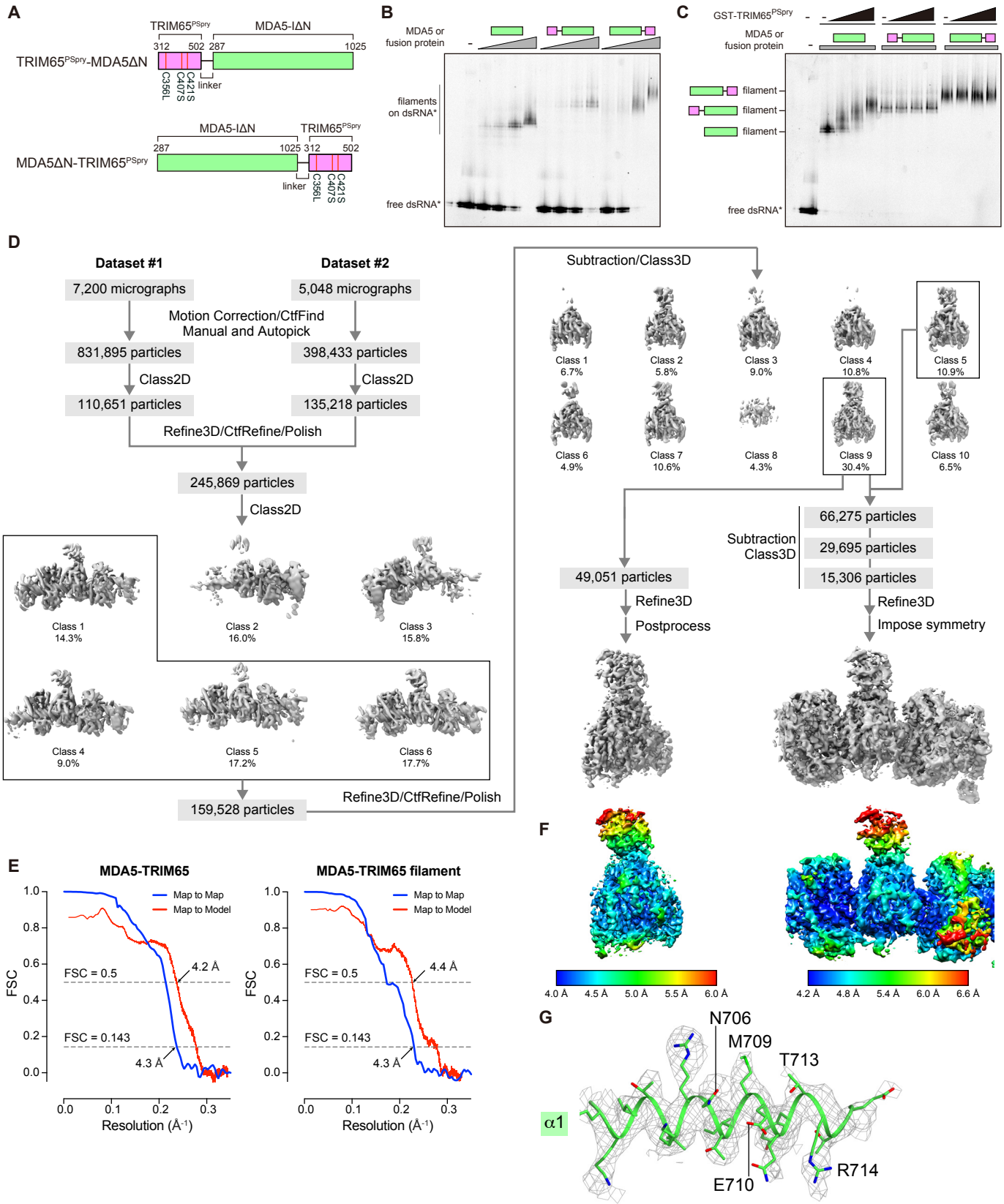

Figure S2. Cryo-EM data processing for the TRIM65PSpry:MDA5ΔN complex, Related to Figure 2

(A) Schematic of TRIM65PSpry fused with MDA5ΔN at the N- or C-terminus. The 38 amino acid linker was derived from the multi-cloning site of pET50b vector. Three Cys (C356, C407 and C421) in TRIM65PSpry were mutated to improve the protein stability.

(B) Filament formation of MDA5ΔN, TRIM65PSpry-MDA5ΔN and MDA5ΔN-TRIM65PSpry on 112 bp dsRNA. The mobility shift of Cy5-labeled (*) dsRNA (1 ng/μl) was monitored by native PAGE with an increasing concentration (62.5, 125, 250 and 500 nM) of MDA5ΔN or the fusion proteins. Cy5 fluorescence was used for gel imaging.

(C) GST-PSpry binding assay. Filaments of MDA5ΔN, TRIM65PSpry-MDA5ΔN and MDA5ΔN-TRIM65PSpry were formed on Cy5-labeled (*) 112 bp dsRNA as in (b) and their mobilities were monitored by PAGE with an increasing concentration (72.5, 150 and 300 nM) of GST-TRIM65PSpry.

(D) Cryo-EM image processing workflow (see details in STAR Methods).

(E) Fourier shell correlation (FSC) curve for the monomeric (left panel) and filamentous (right panel) MDA5:TRIM65 complex. Map-to-Map FSC curve was calculated between the two independently refined half-maps after masking (blue line), and the overall resolution was determined by gold standard FSC=0.143 criterion. Map-to-Model FSC was calculated between the refined atomic models and maps (red line).

(F) Local resolution for the maps of the monomeric (left panel) and filamentous (right panel) MDA5:TRIM65 complex. Local resolution was calculated by Relion, and resolution range was indicated according to the color bar.

(G) Cryo-EM density map for the α1 helix of MDA5.

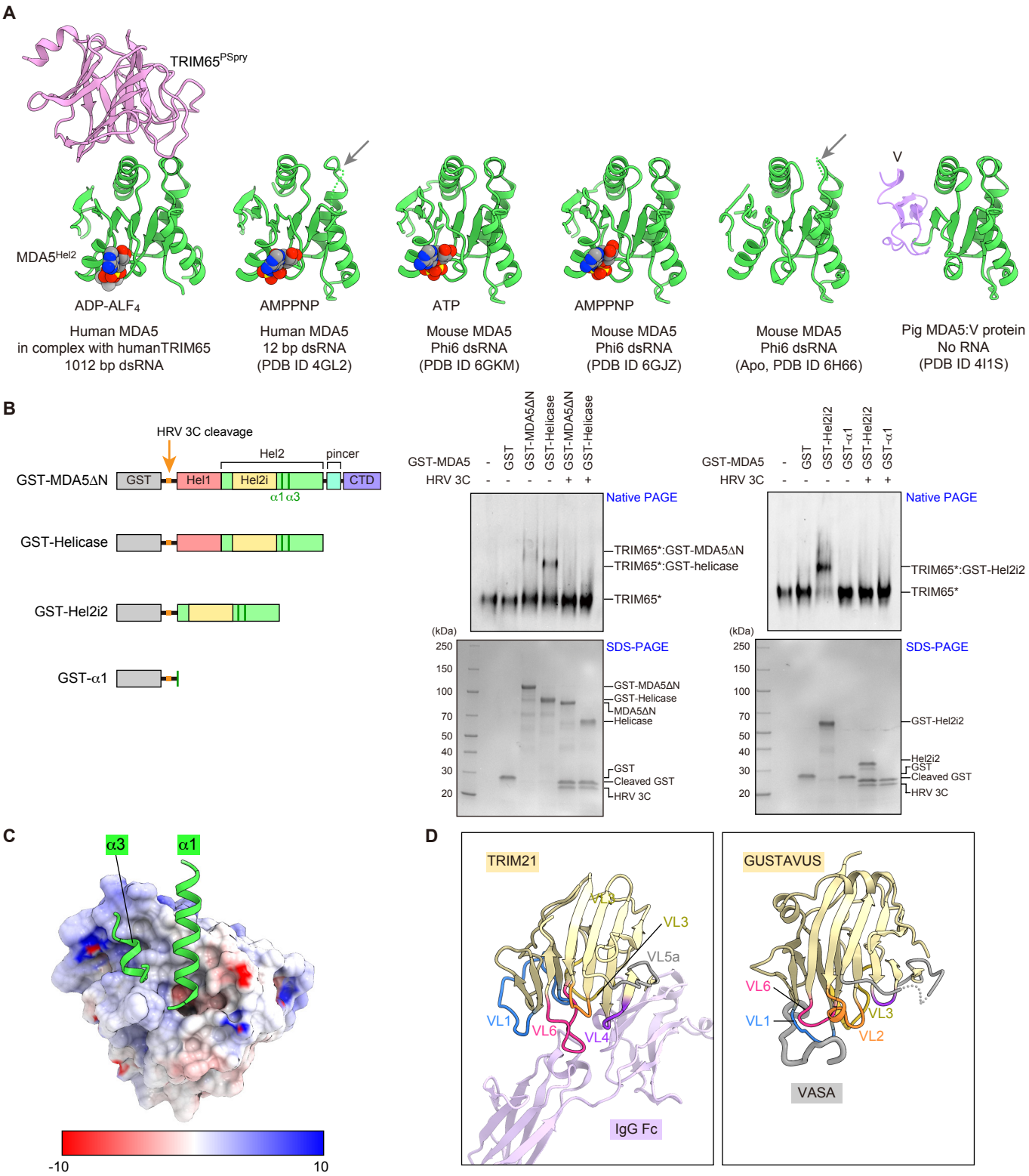

Figure S3. Analysis of the MDA5:TRIM65 complex structure, Related to Figure 2

(A) Comparison of the MDA5 Hel2 structures in the filamentous state with dsRNA and TRIM65 (left, this study), in the monomeric state with dsRNA (center, PDB: 4GL2, RMSD of 1.41 Å compared to the Hel2 in complex with TRIM65), in the filamentous state with dsRNA (PDB: 6GKM, 6GJ2 and 6H66, RMSD of 1.35 Å, 1.40 Å, 1.54 Å, respectively) and in complex with the viral protein V without dsRNA (PDB: 4I1S, RMSD of 1.09 Å). ATP or ATP analogues are shown in sphere models. Disordered regions on α3 are indicated by grey arrows.

(B) Native gel shift assays to examine the interaction between MDA5 and TRIM65 in the absence of dsRNA. TRIM65 was N-terminally labeled with fluorescein (*) for visualization in the native gel. Mobility shift of TRIM65 (CC-PSpry, 0.8 μM) was monitored upon incubation with MDA5 fused with GST (GST-MDA5, 1.6 μM). Various MDA5 constructs were used to confirm the interaction between MDA5Hel2 and TRIM65: MDA5ΔN, helicase domain, Hel2i-Hel2 (Hel2i2) and isolated α1 helix. Note that isolated Hel2 could not be tested due to its insolubility. We instead used Hel2i2, which was soluble. The GST tag is cleavable by the HRV 3C protease, allowing comparison of the MDA5:TRIM65 interaction in the monomeric (without GST) vs. dimeric (with GST) states. The results showed that MDA5ΔN, helicase domain and Hel2i2 all bind TRIM65 in a manner dependent on GST fusion. Isolated α1 helix did not bind TRIM65, with or without GST, suggesting that α3 is also required. All proteins were recombinantly expressed in E. coli and purified to homogeneity. Bottom: Input samples analyzed by SDS-PAGE and Coommassie Brilliant Blue (CBB) stain.

(C) Electrostatic potential of TRIM65PSpry in surface representation. The α1/α3 helices of MDA5ΔN bound by TRIM65PSpry are shown in ribbon representation (green).

(D) Structures of other PSpry domains in complex with their respective substrates. Left: TRIM21PSpry in complex with IgG Fc (PDB:2IWG (James et al., 2007)). Right: GUSTAVUSPSpry in complex with a peptide isolated from VASA (PDB:2IHS (Woo et al., 2006)). VLs involved in substrate recognition are indicated by VL labels. TRIM21PSpry utilizes VL1 and 3-6 to recognize a domain-domain interface of the IgG antibody, whereas GUSTAVUSPSpry utilizes VL1-3 and 6 to recognize a linear peptide in VASA. Note that VASA is a helicase, but the PSpry epitope resides outside the helicase domain.

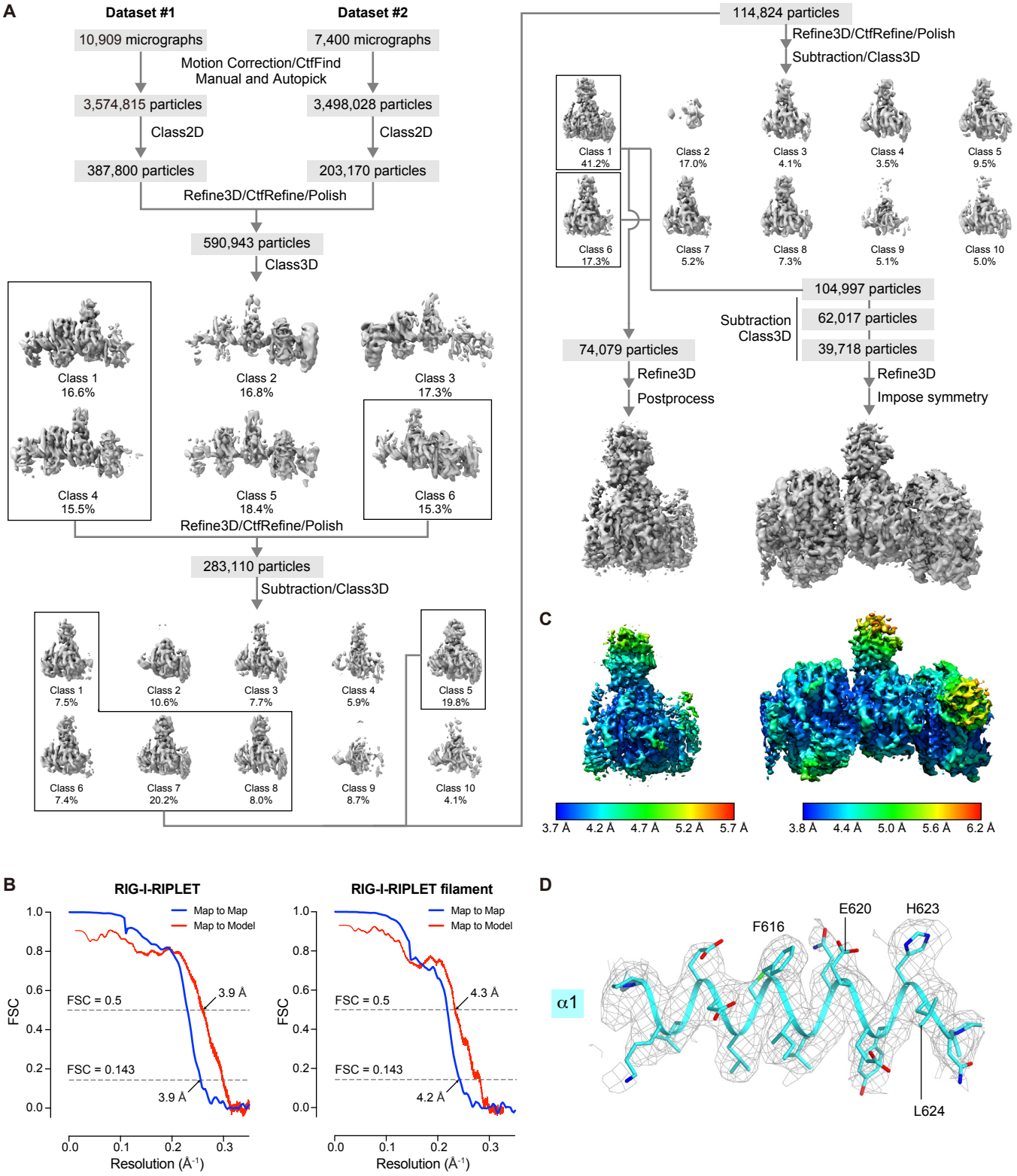

Figure S4. Cryo-EM data processing for the RIPLETPSpry:RIG-I∆N complex, Related to Figure 3

(A) Cryo-EM image processing workflow (see details in STAR Methods).

(B) Fourier shell correlation (FSC) curve for the monomeric (left panel) and filamentous (right panel) RIG-I:RIPLET complex. Map-to-Map FSC curve was calculated between the two independently refined half-maps after masking (blue line), and the overall resolution was determined by gold standard FSC=0.143 criterion. Map-to-Model FSC was calculated between the refined atomic models and maps (red line).

(C) Local resolution for the maps of the monomeric (left panel) and filamentous (right panel) RIG-I:RIPLET complex. Local resolution was calculated by Relion, and resolution range was indicated according to the color bar.

(D) Cryo-EM density map for the α1 helix of RIG-I.

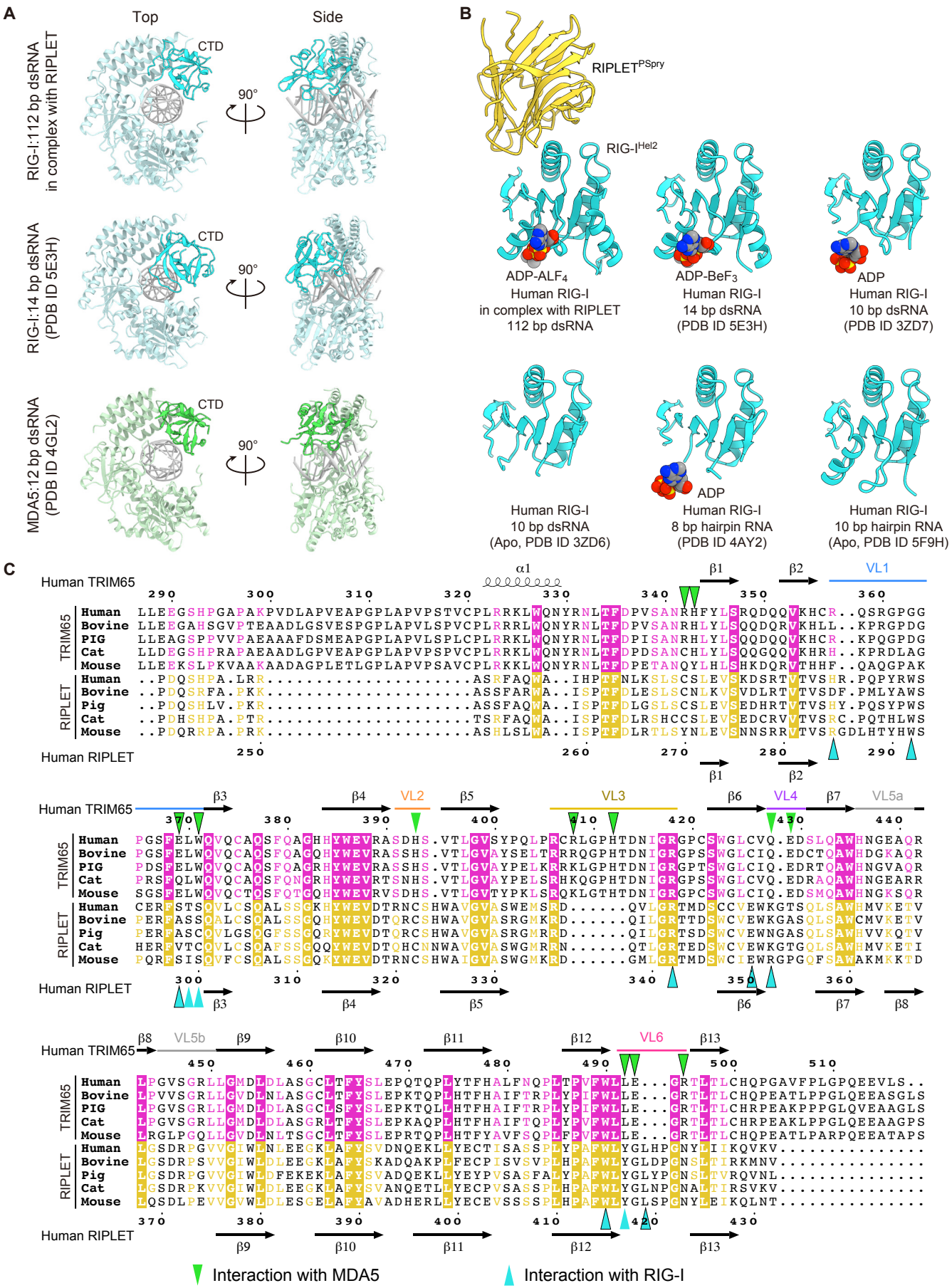

Figure S5. Analysis of the RIG-I:RIPLET complex structure, Related to Figures 3 and 4

(A) Structural comparison of filamentous RIG-I:112 bp dsRNA with monomeric RIG-I:14 bp dsRNA (PDB: 5E3H) and monomeric MDA5:12 bp dsRNA (PDB: 4GL2) in top and side views.

(B) Comparison of the RIG-I Hel2 structures in the filamentous state with dsRNA and RIPLET (this study) and in the monomeric state with dsRNA (PDB: 5E3H, 3ZD7, 3ZD6, 4AY2 and 5F9H, RMSD of 1.15 Å, 1.36 Å, 1.35 Å, 1.16 Å and 1.15 Å, respectively). ATP or ATP analogues are shown in sphere models.

(C) Sequence alignment of orthologs of TRIM65 and RIPLET near the MDA5/RIG-I interface. Residues involved in the interaction with MDA5 and RIG-I are indicated with triangles. Sequences were aligned using Clustal Omega (http://www.ebi.ac.uk/Tools/msa/clustalo), and alignment figures were generated using ESPript3 (http://espript.ibcp.fr/ESPript/ESPript).

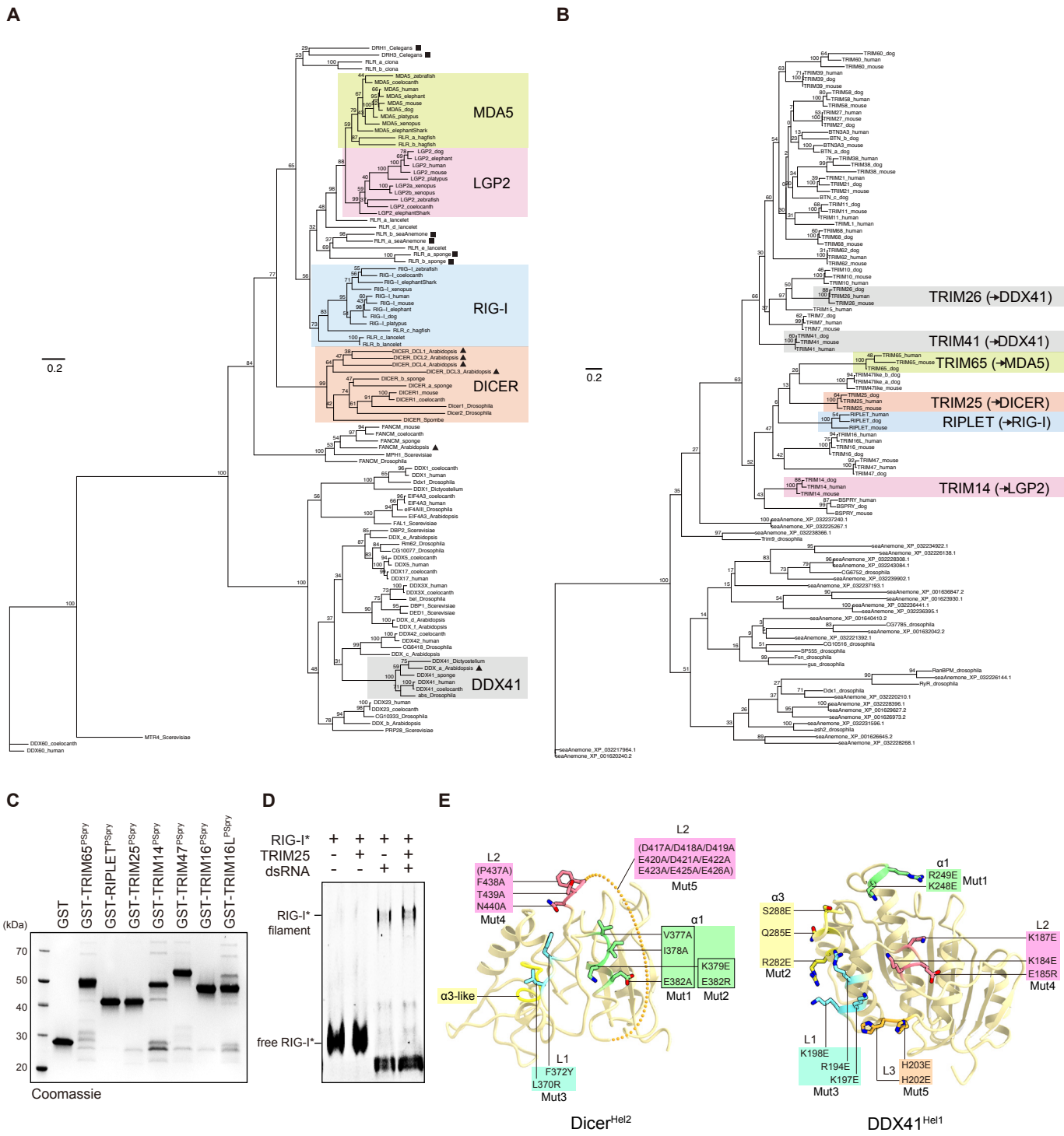

Figure S6. Analysis of related helicases and PSpry/Spry-containing proteins, Related to Figures 5 and 6

(A) Phylogenetic trees of selected helicases and PSpry/Spry-containing proteins. The helicase domain phylogeny includes human representatives of the RLRs and their closest relatives DICER and FANCM, a number of DEAD-box helicases, and the outgroup DDX60, a Ski2-like helicase, for rooting. We added selected orthologs chosen to help put lower bound estimates on the age of the duplication events that gave rise to these diverse helicases. Because the plant Arabidopsis thaliana has clear orthologs (triangles) of human DDX41, FANCM and DICER, these genes must have diverged from one another in or before the common ancestor of all eukaryotes >1500 million years ago (mya) (Kumar et al., 2017). While we have not identified a plant ortholog for RIG-I/MDA5/LGP2, these proteins group with several C. elegans, Nematostella vectensis (sea anemone) and Amphimedon queenslandica (sponge) sequences (squares), indicating that they diverged from DICER >950mya (Zou et al., 2009). The scale bars represent 0.2 amino acid substitutions per site. Numbers at each node show bootstrap values (100 replicates).

(B) The PSpry/Spry-domain phylogeny includes all TRIM proteins studied functionally in this manuscript and their close relatives, including human, dog and mouse orthologs where available. It is not intended to be a comprehensive TRIM phylogeny. We added all alignable Spry-containing proteins from Drosophila melanogaster and Nematostella vectensis (sea anemone) and display the tree with arbitrary rooting. Because the studied TRIM proteins group together to the exclusion of Drosophila and Nematostella sequences, we infer that the duplications giving rise to these TRIM proteins occurred <800mya. Interacting helicases are shown in parenthesis. The scale bars represent 0.2 amino acid substitutions per site. Numbers at each node show bootstrap values (100 replicates)

(C) SDS-PAGE analysis of recombinant GST-PSpry proteins used in Figure 5A.

(D) Native gel mobility shift assays to test RIG-I:TRIM25 interaction. Fluorescein-labeled (*) full-length RIG-I (600 nM) was incubated with TRIM25 (300 nM) in the presence and absence of 112 bp dsRNA (4 ng/μl). Fluorescein fluorescence was used for gel imaging. The result shows no binding between RIG-I and TRIM25, with or without dsRNA.

(E) Mutations in Dicer and DDX41 used in Figure 6B-D. Mutated residues are mapped onto the structures of human Dicer Hel2 (PDB:5ZAL) and human DDX41 Hel1 (PDB:5GVR).